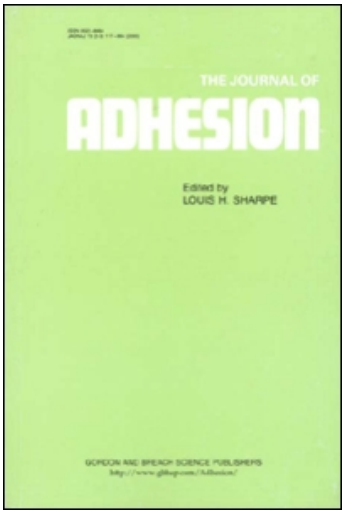

The Journal of Adhesion
Publication details, including instructions for authors and subscription information:
http://www.informaworld.com/smpp/title~content=t713453635

Influence of Fabrication Residual Thermal Stresses on Rubber-toughened Adhesive Tubular Single Lap Steel-Steel Joints under Tensile Load

Young Goo Kim[a]; Dai Gil Lee[a]
[a] Department of Mechanical Engineering, Korea Advanced Institute of Science and Technology, Yusong-gu, Taejon-shi, Korea

To cite this Article Kim, Young Goo and Lee, Dai Gil(1998) 'Influence of Fabrication Residual Thermal Stresses on Rubber-toughened Adhesive Tubular Single Lap Steel-Steel Joints under Tensile Load', The Journal of Adhesion, 65: 1, 163 — 185
To link to this Article: DOI: 10.1080/00218469808012244
URL: http://dx.doi.org/10.1080/00218469808012244

J. Adhesion, 1998, Vol. 65, pp. 163- 185
Reprints available directly from the publisher
Photocopying permitted by license only

Influence of Fabrication Residual Thermal Stresses on Rubber-toughened Adhesive Tubular Single Lap Steel-Steel Joints under Tensile Load

YOUNG GOO KIM and DAI GIL LEE*

Department of Mechanical Engineering, Korea Advanced Institute of Science and Technology, ME3221, Gusong-dong, Yusong-gu, Taejon-shi, Korea 305-701

(Received 5 December 1996; In final form 16 April 1997)

The tensile load bearing capability of adhesively-bonded tubular single lap joints which is calculated under the assumption of linear mechanical adhesive properties is usually much less than the experimentally-determined because the majority of the load transfer of adhesively-bonded joints is accomplished by the nonlinear behavior of rubber-toughened epoxy adhesives. Also, as the adhesive thickness increases, the calculated tensile load bearing capability with the linear mechanical adhesive properties increases, while, on the contrary, the experimentally-determined tensile load bearing capability decreases.

In this paper, the stress analysis of adhesively-bonded tubular single lap steel-steel joints under tensile load was performed taking into account the nonlinear mechanical properties and fabrication residual thermal stresses of the adhesive. The nonlinear tensile properties of the adhesive were approximated by an exponential equation which was represented by the initial tensile modulus and ultimate tensile strength of the adhesive.

Using the results of stress analysis, the failure criterion for the adhesively-bonded tubular single lap steel-steel joints under tensile load was developed, which can be used to predict the load-bearing capability of the joint. From the failure criterion, it was found that the fracture of the adhesively-bonded joint was much influenced by the fabrication residual thermal stresses.

Keywords: Adhesively bonded tubular single lap joint; nonlinear mechanical property; tensile load bearing capability; nonlinear exponential approximation; fabrication residual thermal stress; failure criterion

*Corresponding author.

INTRODUCTION

The design of joints for the assembly of seperated parts has become an important research area because the structural efficiency of a structure with joints is established, with very few exceptions, by its joints, not by its basic structures.

There are two kinds of joints, *i.e.* mechanical and adhesively-bonded for composite structures. The mechanical joints is created by fastening the substrates with bolts or rivets, but the adhesively-bonded joint uses an adhesive interlayer between the adherends.

The adhesively-bonded joint can distribute load over a larger area than the mechanical joint, requires no holes, adds very little weight to the structure and has superior fatigue resistance [1,2]. However, the adhesively-bonded joint requires careful surface preparation of the adherends, is affected by service environments and is difficult to disassemble for inspection and repair.

There are several types of tubular lap lap joints, such as the single lap joint, the double lap joint, the stepped lap joint, and the scarf lap joint. Of these, the tubular single lap joint is most popular, due to its ease of manufacture and its relatively low cost.

Stress analyses of adhesively-bonded tubular single lap joints under axial load have been conducted by several researchers through analytical and finite element methods [3–9]. Lubkin and Reissner [3] assumed that the adhesive thickness was much less than the adherend thickness and that the adherend thickness was much less than the radius of the tubular joint, from which they applied thin shell theory to the joint analysis. They modelled the adhesive layer as an infinite number of coil springs with the assumption that the adhesive was much softer than the adherend. Adams and Peppiatt [4] refined the solution of Volkersen and gave a closed-form solution for the shear stresses of the adhesively-bonded tubular single lap and partially-tapered tubular scraf lap joints. They also analyzed adhesively-bonded tubular single lap joints which were subjected to axial and torsional loads using the finite element method when the adhesive had a fillet. Griffin *et al.* [5] proposed a strength model which could predict the fracture of the adhesively-bonded single lap joint under tensile loads. Shi and Cheng [6] proposed an approximate closed from solution for the stress distributions in the adhesive and adherends when the

adhesively-bonded lap joints were under tensile loads. Terekhova and Skoryi [7] proposed a closed form solution for adhesively-bonded lap joints under tensile loads and internal pressure. They applied thin shell theory to the joint analysis. Kukovyakin and Skoryi [8] proposed a closed form solution for the adhesively-bonded bushing-shaft type joint under tensile loads. They considered that the bushings were thin-walled and deformed in accordance with the moment theory of thin-walled shells. Harrison and Harrison [9] developed a simple method for calculating the stresses near the ends of a parallel-sided adhesive layer.

In the majority of the past studies the linear elastic shear properties of the adhesive have been used in the stress analysis of the adhesively-bonded tubular single lap joint. However, the adhesive under load usually experiences large plastic deformation before the onset of adhesive fracture and, consequently, the majority of the load transfer of the adhesively-bonded joint is accomplished by the region of nonlinear plastic behavior of the adhesive [10]. Kim *et al.*, proposed a failure model for adhesively-bonded tubular single lap steel-steel joints with nonlinear mechanical properties and fabrication residual thermal stresses. The nonlinear tensile stress-strain relationship of the adhesive was modelled by a two-parameter exponential equation that was represented by the initial tensile modulus and ultimate tensile strength of the adhesive [11].

In this paper, the nonlinear mechanical properties modeled by the two-parameter exponential equation and the fabrication residual thermal stresses of the adhesive were taken into consideration in the stress analyses of an adhesively-bonded tubular single lap joints with steel-steel adherends. The initial tensile modulus and ultimate tensile strength of the adhesive were obtained by a tensile test.

In this work, the tensile load on the adhesive joint was varied from 5 kN to 25 kN and the stress distributions in the adhesive of adhesively-bonded tubular single lap joints were obtained. The stress distributions were calculated for four different adhesive properties: (case 1) nonlinear mechanical property with residual thermal stresses of the adhesive; (case 2) linear mechanical property with residual thermal stresses of the adhesive; (case 3) nonlinear mechanical property without residual thermal stresses of the adhesive; (case 4) linear mechanical property without residual thermal stresses of the adhesive.

From the results of the stress analyses, the fracture intensity index which could predict the fracture of the joint was defined and calculated using a failure model [12] for the adhesively-bonded tubular single lap steel-steel joints under axial loads. Finally, the failure indices obtained from the stress analyses were compared with those obtained from experiments to assess the influence of the fabrication thermal stresses on the adhesively-bonded tubular single lap steel-steel joints.

NONLINEAR MECHANICAL PROPERTIES OF THE RUBBER-TOUGHENED ADHESIVE

The adhesive used in this work was IPCO 9923 rubber-toughened epoxy manufactured by the Imperial Polychemicals Corporation (Azusa, California, USA) which had high shear and peel strength. Table I shows the material properties of the adhesive.

The nonlinear mechanical properties of the adhesive were modelled by the following exponential form:

$$\sigma = \sigma_m(1 - e^{-(E_0/\sigma_m)\varepsilon}) \tag{1}$$

where σ is the tensile stress in the adhesive, σ_m the ultimate tensile strength of the adhesive, E_0 the initial Young's modulus and ε the tensile strain in the adhesive. Figure 1 shows the tensile stress-strain relations of the adhesive determined by the test method of ASTM D 638-89 as well as by Eq. (1).

The shear strength and plastic characteristics of the epoxy adhesive were obtained by the bulk shear test.

TABLE I Properties of the epoxy adhesive and the steel adherend

	Adhesive (IPCO 9923)	*Steel*
Tensile modulus (GPa)	1.30	207.0
Poisson's ratio	0.41	0.30
Tensile strength (MPa)	45.0	not required
Shear strength (MPa)	29.5	not required
Shear strain limit	0.60	not required
C. T. E. (10^{-6}m/m°C)	72.0	11.7
Viscosity	paste type	not applicable
Cure temperature (°C)	80.0	not applicable
Cure time (hour)	4	not applicable

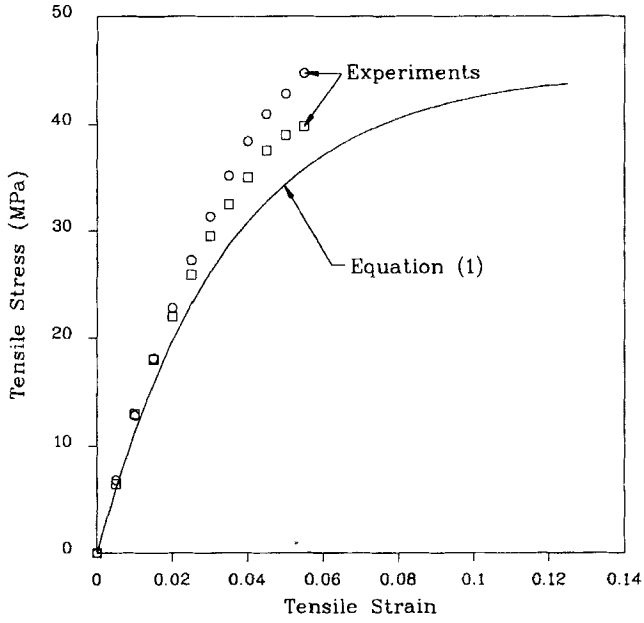

FIGURE 1 Tensile Stress-Strain Relations of the Epoxy Adhesive (IPCO 9923).

Figure 2 shows the shear stress-strain relations of the adhesive obtained from the bulk shear test of the adhesive and the multi-linear function calculated using the two-parameter nonlinear exponential Eq. (1) and Poisson's ratio. Assuming that the nonlinear tensile property of the adhesive in an infinitesimal shear strain range was linear, the shear modulus of the adhesive was calculated using the elastic modulus and Poisson's ration. Using the shear modulus of the adhesive calculated in the infinitesimal range, the shear stress-strain curve was obtained. Since the epoxy adhesive used in this work was rubber-toughened, it revealed very large plastic strain, especially in the shear mode, as shown in Figure 2.

EXPERIMENTS

The finite element calculation with the assumption of the linear elastic properties of the adhesive predicted that the load-bearing capability

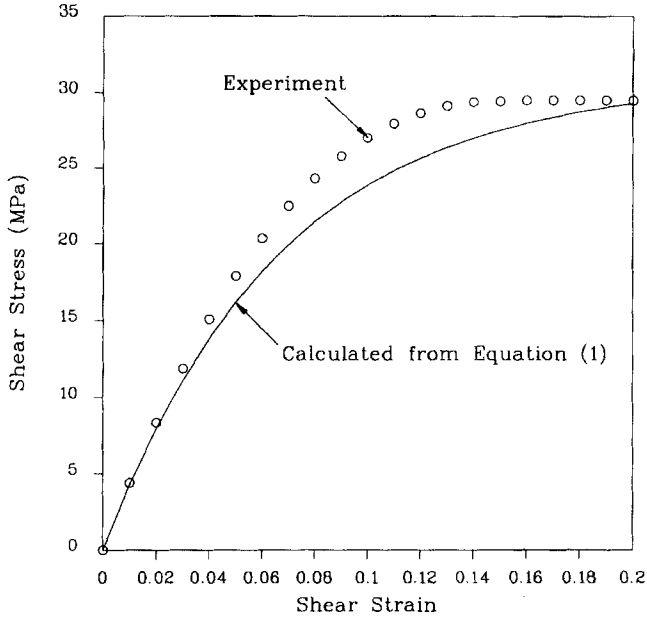

FIGURE 2 Shear Stress-Strain Relations of the Epoxy Adhesive (IPCO 9923).

of the adhesively-bonded joint increased as the adhesive thickness increased [4], which was contrary to the experimental result. In reality, the load-bearing capability of the adhesively-bonded joint decreases as the adhesive thickness increases because the fabrication residual thermal stresses originating from the cure of the adhesive lower the fracture strength of the adhesive [11].

Figure 3 shows the adhesively-bonded tubular single lap joint with steel-steel adherends which was tested in this work. The bonding length was 20 mm and the adhesive thickness of the joint was adjusted by changing the outer diameter of the inner adherend while the inner diameter of the outer adherend was fixed. The outer and inner diameters of the outer adherend were 21 mm and 17 mm, respectively. The tensile load bearing capabilities of the joints were measured when the adhesive thickness varied from 0.05 mm to 1.0 mm.

Both the inner and outer adherends have precisely ground surfaces which were mounted on a precise V-block during the cure of the adhesive for concentric bonding. An arithmetic surface roughness of 2 μm was chosen for the adherend surface roughness because this

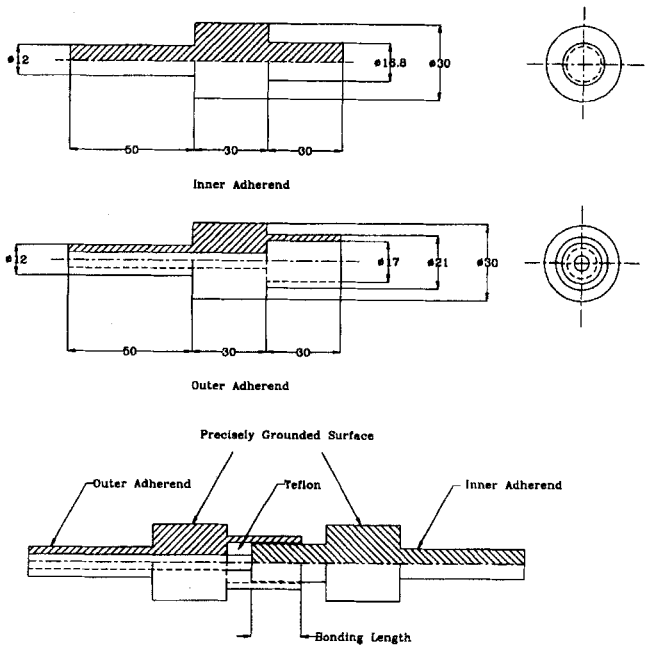

FIGURE 3 Configuration of the adhesively-bonded joint specimen.

value was proved to be the optimum for the fatigue strength of the adhesively-bonded tubular single lap joint [12]. The adhesively-bonded joints were cured in an autoclave for 4 hours under a temperature 80°C and a pressure 0.6 Mpa.

STRESS ANALYSIS BY FINITE ELEMENT METHOD

Carpenter [13] compared the stresses obtained from the finite element analysis of lap joints with the results from the consistent lap joint theory. He modeled the adherend with beam elements and the adhesive with four-node isoparametric elements. He concluded that the one layer of four-node isoparametric elements for the adhesive gave results close to the consistent lap joint theories. To compare the results obtained by Carpenter, the adhesive layer was modeled with one-, two- and three-layer four-node isoparametric elements, respectively, and found that they gave almost the same results.

Figure 4 shows the finite element mesh for the adhesive and the steel adherends in which the four-node isoparametric elements were used. The number of nodes and elements were 1025 and 950, respectively. The tensile load range for the stress analysis of the adhesively-bonded joints was from 5 kN to 25 kN.

Five uniformly-spaced elements were used along the adhesive thickness because the variation of the stresses was not large through the adhesive thickness. Fifty elements were used along the adhesive length and the size of elements was decreased toward the ends of the adhesive taking into consideration the stress concentration. However, the stresses at the interface of the adhesive were artifical because the stresses were calculated at the Gauss points rather than at the interface.

The residual thermal stresses of the adhesive due to temperature difference were calculated by taking into consideration the coefficients of thermal expansion of the adherends and adhesive. The temperature difference, ΔT, between curing and testing was 60°C in (case 1) and (case 3), and was 0°C in (case 2) and (case 4) for the analysis of residual thermal stresses.

The coefficients of thermal expansion of the adherends and the epoxy adhesive between the curing and testing temperature were assumed to be linear with respect to the temperature difference.

Also, to know the effect of the initial residual thermal stresses on the adhesively-bonded joints, the initial residual thermal stresses

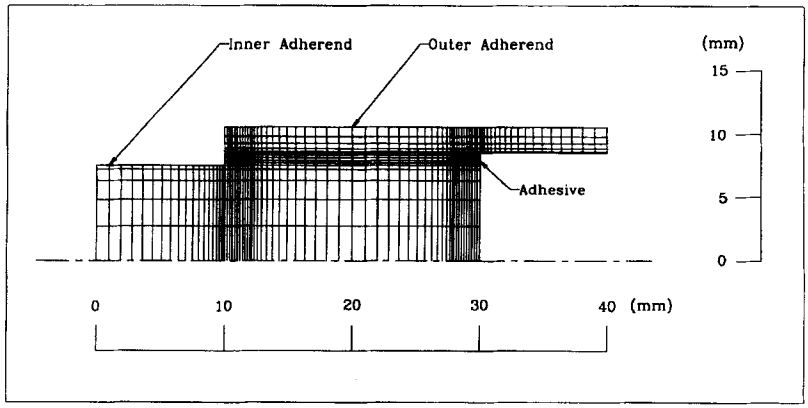

FIGURE 4 Finite element mesh for stress analysis.

originating from the temperature difference during the cure of adhesive were calculated. The curing temperature of the adhesive joint was 80°C and the test temperature was 20°C.

FAILURE MODEL OF THE ADHESIVE WITH RESPECT TO LOADS

It was assumed that the bonding strength between the adhesive and the adherend was not larger than the adhesive bulk shear strength because the residual tensile thermal stresses were produced due to the temperature difference during the curing of the adhesive. Therefore, the failure index in this analysis was applied at the adhesive elements which were in contact with the elements of the inner adherend.

In order to predict the failure condition of the adhesively-bonded joint, the nondimensional failure index, k, was defined by the following equation [14].

$$k = \sqrt{\left(\left(\frac{\sigma_{rr}}{S_T}\right)^2 + \left(\frac{\sigma_{\theta\theta}}{S_T}\right)^2 + \left(\frac{\sigma_{zz}}{S_T}\right)^2 + \left(\frac{\tau_{rz}}{S_S}\right)^2 + \left(\frac{\tau_{r\theta}}{S_S}\right)^2 + \left(\frac{\tau_{z\theta}}{S_S}\right)^2\right)} \quad (2)$$

where,

S_T : bulk tensile strength of the adhesive
S_S : bulk shear strength of the adhesive
σ_{rr} : radial stress in the adhesive
$\sigma_{\theta\theta}$: hoop stress in the adhesive
σ_{zz} : axial stress in the adhesive
τ_{rz} : shear stress in the adhesive
$\tau_{r\theta}$: shear stress in the adhesive
$\tau_{z\theta}$: shear stress in the adhesive

From Eq. (2), the initial failure index, k_I, due to temperature difference only was calculated as follows:

$$k_I = \sqrt{\left(\left(\frac{\sigma_{rr}^T}{S_T}\right)^2 + \left(\frac{\sigma_{\theta\theta}^T}{S_T}\right)^2 + \left(\frac{\sigma_{zz}^T}{S_T}\right)^2 + \left(\frac{\tau_{rz}^T}{S_S}\right)^2\right)} \quad (3)$$

where,

σ_{rr}^T : radial residual thermal stress in the adhesive
$\sigma_{\theta\theta}^T$: hoop residual thermal stress in the adhesive
σ_{zz}^T : axial residual thermal stress in the adhesive
τ_{rz}^T : shear residual thermal stress in the adhesive

In reference [11], the fracture intensity index when the joint failed was proposed as follows:

$$k_F \equiv \sqrt{1 - k_I^2} \tag{4}$$

In this work, the failure index in the adhesive elements which were in contact with the inner adherend was calculated.

Figure 5 shows the initial failure index, k_I, with respect to the adhesive thickness calculated using Eq. (3). In Figure 4, the initial failure index, k_I, increased as the adhesive thickness increased because the

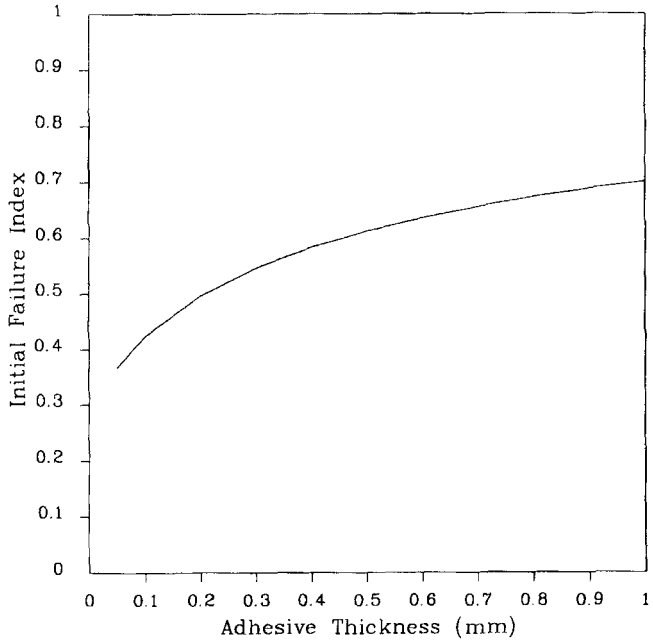

FIGURE 5 Initial failure index, k_I, of the adhesively-bonded joint due to the fabrication residual thermal stresses caused by the temperature difference of 60°C between curing the testing, with respect to the adhesive thickness.

thermal stress components increased as the adhesive thickness increased.

Figure 6 shows the load-bearing capability of the adhesively-bonded tubular single lap steel-steel joint obtained from the experiment and the curve fitting of Figure 5 for the stress analyses.

Figure 7 shows the fracture intensity index, k_F, obtained from Eq. (4) and the maximum failure index, k_{max}, calculated from Eq. (2) using the curve-fitted load-bearing capability obtained from the experiment, with respect to the adhesive thickness.

In Figure 6, the fracture intensity index, k_F, decreased as the adhesive thickness increased. The decrease of the fracture intensity index, k_F, was caused by the increase of all the fabrication residual thermal stress components. The value of k_F was almost the same as that of the maximum failure index, k_{max}, calculated with the nonlinear mechanical properties and fabrication residual thermal stresses of the adhesive.

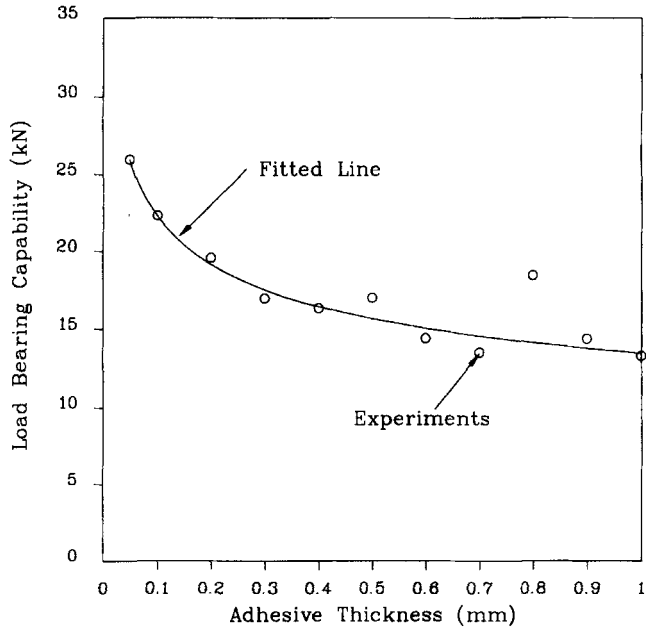

FIGURE 6 Measured static load-bearing capability of the adhesively-bonded tubular single lap joint.

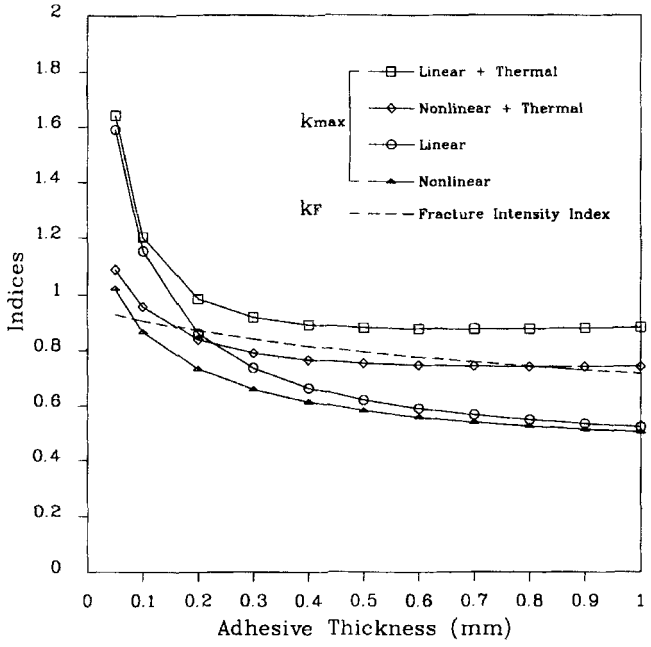

FIGURE 7 Fracture intensity index, k_F, and maximum failure index, k_{max}, obtained from the load-bearing capability and the stress analyses for the adhesively-bonded joint, with respect to the adhesive thickness.

Therefore, it was proposed that the failure of the adhesively-bonded joint occurred when the maximum failure index, k_{max}, calculated with nonlinear mechanical properties and fabrication residual thermal stresses of the adhesive, was larger than the fracture intensity index, k_F.

Figure 8 shows k_{max} and k_F, calculated using Eqs. (3) and (4) with respect to the adhesive thickness with linear mechanical properties and without residual thermal stresses of the adhesive, when the tensile load varied from 5 kN to 25 kN.

Figure 9 shows k_{max} and k_F, calculated using Eqs. (3) and (4) with respect to the adhesive thickness with linear mechanical properties and residual thermal stresses of the adhesive, when the tensile load varied from 5 kN to 25 kN.

Figure 10 shows k_{max} and k_F calculated using Eqs. (3) and (4) with respect to the adhesive thickness with nonlinear mechanical properties and without residual thermal stresses of the adhesive, when the tensile load varied from 5 kN to 25 kN.

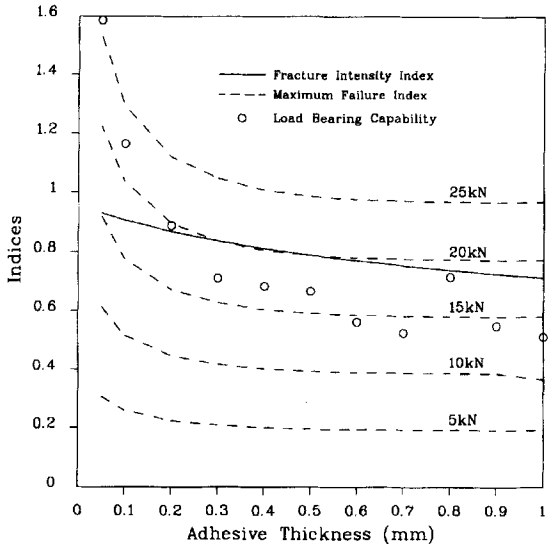

FIGURE 8 Fracture intensity index, k_F, and the maximum failure index, k_{max}, of the adhesively-bonded joint with linear mechanical properties without fabrication thermal stresses of the adhesive, with respect to the adhesive thickness and load variations.

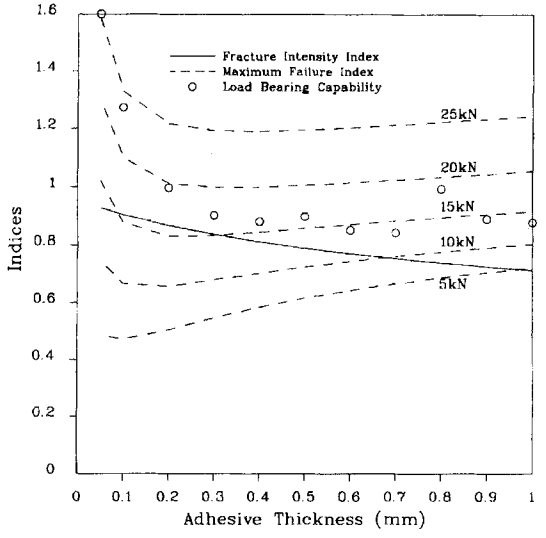

FIGURE 9 Fracture intensity index, k_F, and the maximum failure index, k_{max}, of the adhesively-bonded joint with linear mechanical properties and fabrication thermal stresses of the adhesive, with respect to the adhesive thickness and load variations.

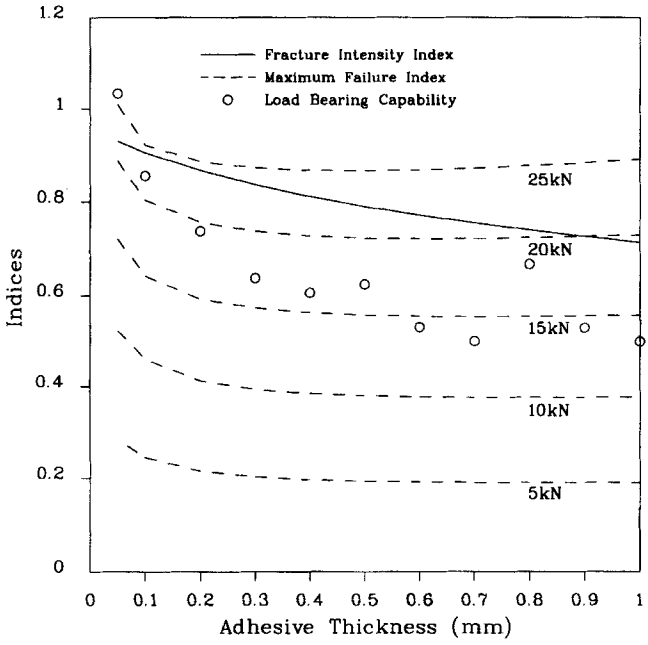

FIGURE 10 Fracture intensity index, k_F, and the maximum failure index, k_{max}, of the adhesively-bonded joint with nonlinear mechanical properties without fabrication thermal stresses of the adhesive, with respect to the adhesive thickness and load variations.

Figure 11 shows k_{max} and k_F calculated using Eqs. (3) and (4) with respect to the adhesive thickness with nonlinear mechanical properties and residual thermal stresses of the adhesive, when the tensile load varied from 5 kN 25 kN.

Comparing Figures 6 and 11, the proposed failure model for the adhesively-bonded joint which predicts joint failure when the maximum failure index is larger than the fracture intensity index, is in good agreement with the experimental results of Figure 6. The calculated load-bearing capabilities were smaller than the experimentally-determined ones when the adhesive thicknesses were smaller than 0.1 mm, but the calculated load-bearing capabilities were almost the same as the experimentally-determined ones when the adhesive thicknesses were larger than 0.1 mm.

From the results of the stress analyses, the failure indices with the linear mechanical property of the adhesive were larger than those with

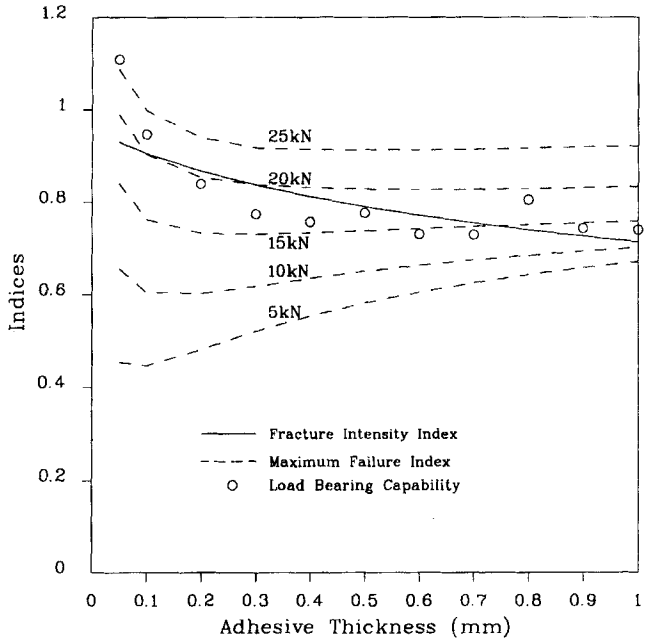

FIGURE 11 Fracture intensity index, k_F, and the maximum failure index, k_{max}, of the adhesively-bonded joint with nonlinear mechanical properties and fabrication thermal stresses of the adhesive, with respect to the adhesive thickness and load variations.

the nonlinear mechanical property of the adhesive. Also, the failure indices with the fabrication residual thermal stresses were larger than the failure indices without the fabrication residual thermal stresses.

As the load was decreased and the adhesive thickness was increased, the failure index calculated with the fabrication thermal stresses was increased. Therefore, in the extreme case of very large adhesive thickness, the failure of the adhesively-bonded tubular single lap steel-steel joint may be caused by the fabrication residual thermal stress only. This fact implies that the fabrication residual thermal stresses caused by the temperature difference between the adhesive curing and room temperatures should be considered in the stress analysis of the adhesively-bonded tubular single lap steel-steel joint.

Figure 12 shows the variations of the radial, hoop, axial and shear stresses due to a temperature difference of only 60°C with respect to adhesive thickness. From the stress analysis, it was found that the

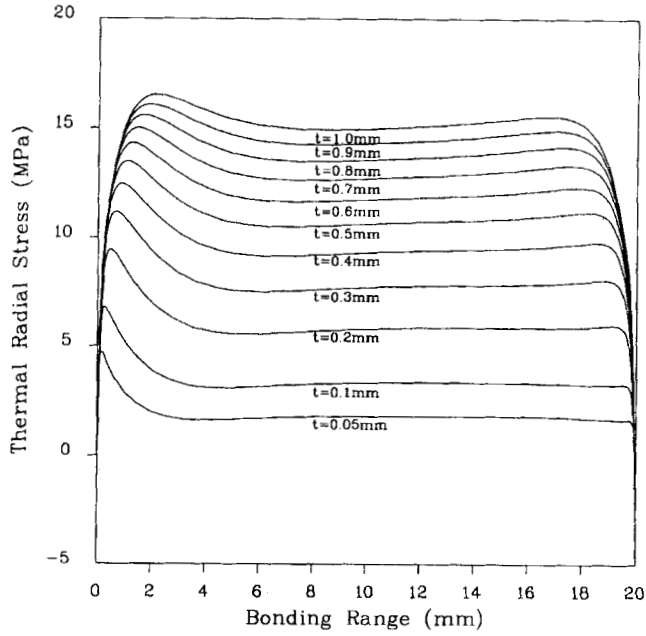

(a)

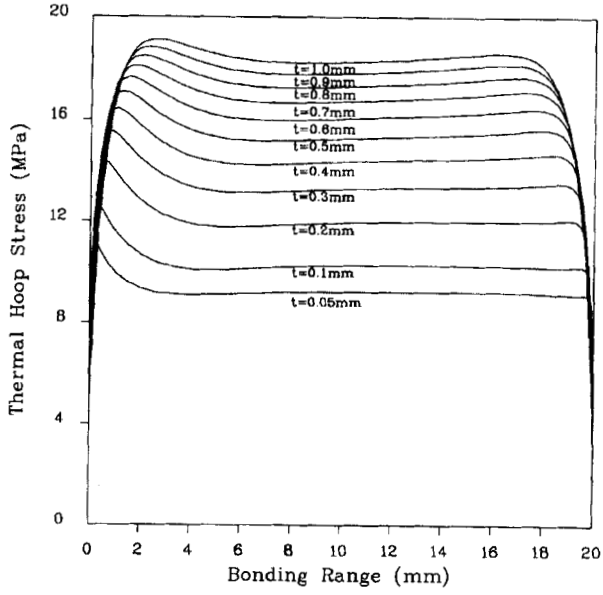

(b)

FIGURE 12 Variations of the fabrication residual thermal stresses due to a temperature difference of 60°C with respect to the adhesive thickness (t: adhesive thickness). (a) Fabrication residual thermal radial stress, (b) Fabrication residual thermal hoop stress, (c) Fabrication residual thermal axial stress, (d) Fabrication residual thermal shear stress.

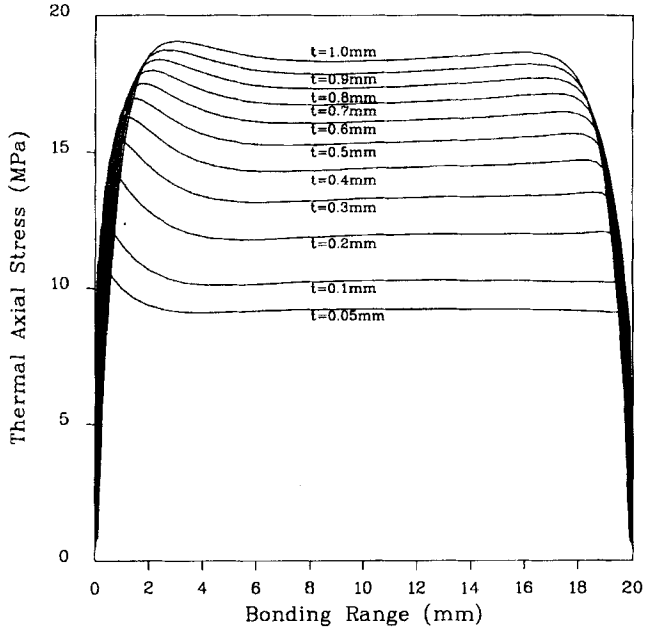

(c)

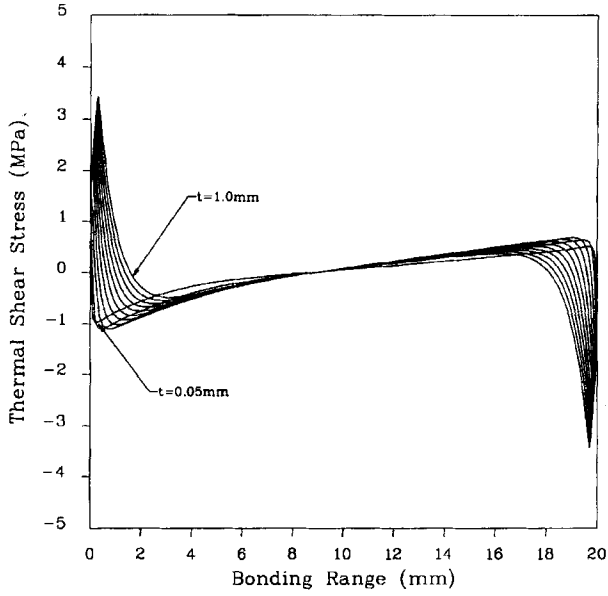

(d)

FIGURE 12 (Continued).

radial, hoop and axial fabrication residual thermal stresses in the adhesive were greatly influenced, but the shear fabrication residual thermal stress was little influenced. Also, as the adhesive thickness increased, the influence of fabrication residual thermal stresses in the adhesive, except for the shear stress, was increased.

Figure 13(a) shows the variation of the initial failure index, k_I, which was produced by a temperature difference of only 60°C and the failure index, k, which was calculated from Eq. (3) with the nonlinear mechanical property and fabrication residual thermal stresses of the adhesive, with respect to the adhesive thickness. The adhesive thickness were 0.05 mm, 0.2 mm, 0.5 mm and 1.0 mm when the tensile axial load was 25 kN.

Figures 13(b) shows the variation of the fracture intensity index, k_F, calculated from Eq. (4) using the initial failure index, k_I, and failure index, k, with the nonlinear mechanical property and fabrication

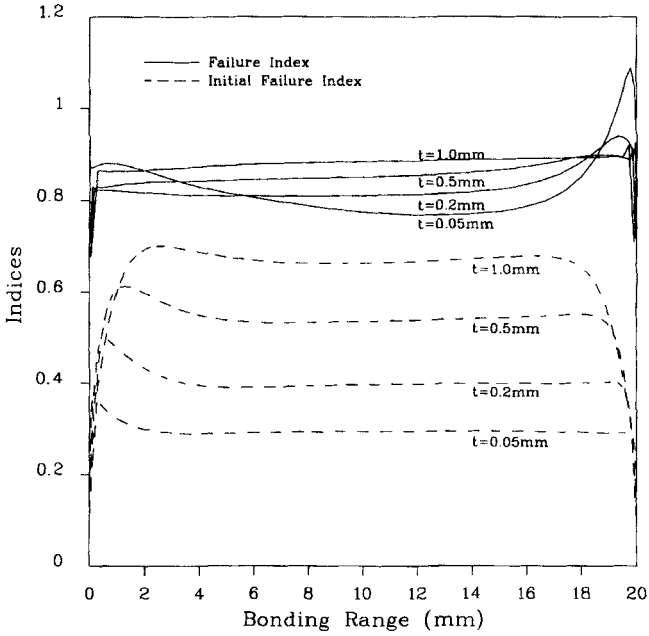

(a)

FIGURE 13 Variations of the initial failure index, k_I, fracture intensity index, k_F, and failure index, k, with respect to the adhesive thickness when the tensile axial load was 25 kN (t: adhesive thickness). (a) Initial failure index, k_I, and failure index, k, (b) Fracture intensity index, k_F, and failure index, k.

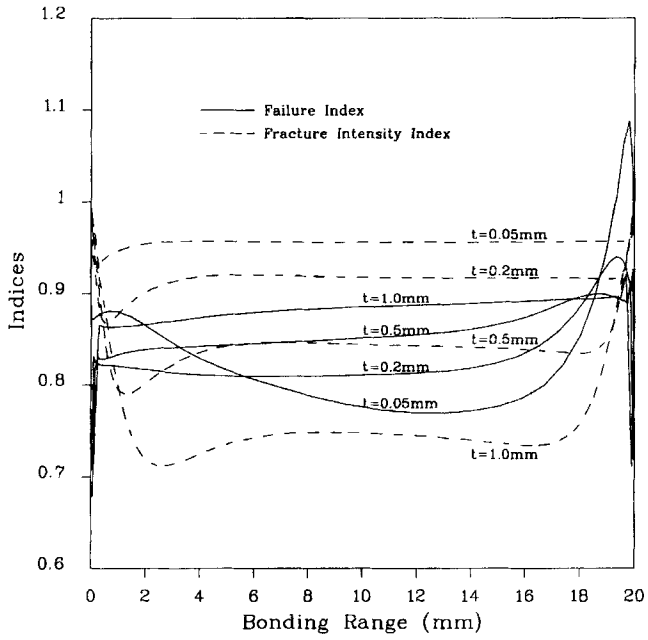

(b)

FIGURE 13 (Continued).

residual thermal stresses of the adhesive. The adhesive thickness were 0.05 mm, 0.2 mm, 0.5 mm and 1.0 mm when the tensile axial load was 25 kN.

Figures 14 and 15 show the variation of k_I, k_F and k with respect to the adhesive thickness when the tensile axial loads were 20 kN and 15 kN, respectively.

From the results of Figure 14 and 15, it was found that k_I increased as the adhesive thickness increased. Since k_F decreased as k_I increased, it was concluded that large values of k_I lowered the load-bearing capability of the adhesively-bonded tubular single lap steel-steel joint under tensile axial load.

In Figures 13 ~ 15, as the adhesive thickness was increased and the load was decreased, the difference between k_I and k was negligible. Therefore, when the adhesive thickness is large, it may be concluded that the failure of the adhesively-bonded single lap joint is caused largely by the fabrication residual thermal stresses of the adhesive.

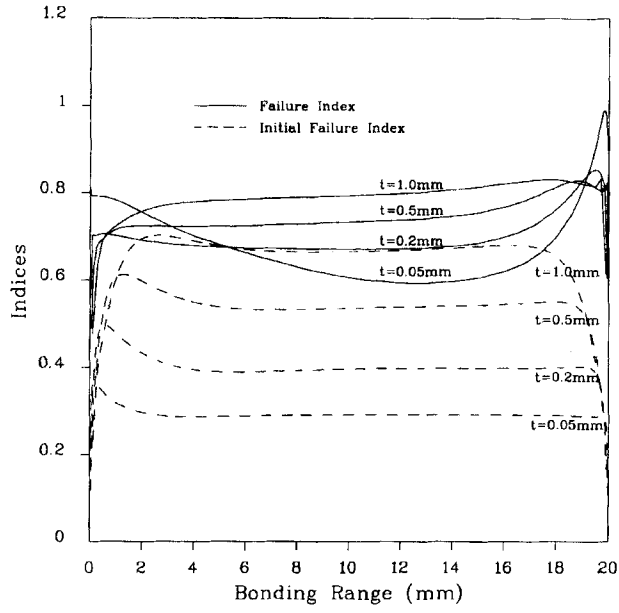

(a)

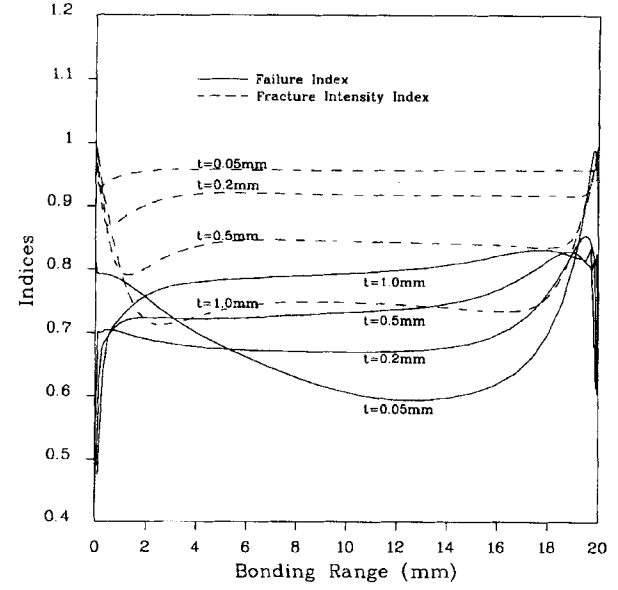

(b)

FIGURE 14 Variations of the initial failure index, k_I, fracture intensity index, k_F, and failure index, k, with respect to the adhesive thickness when the tensile axial load was 20 kN (t: adhesive thickness). (a) Initial failure index, k_I, and failure index, k, (b) Fracture intensity index, k_F, and failure index, k.

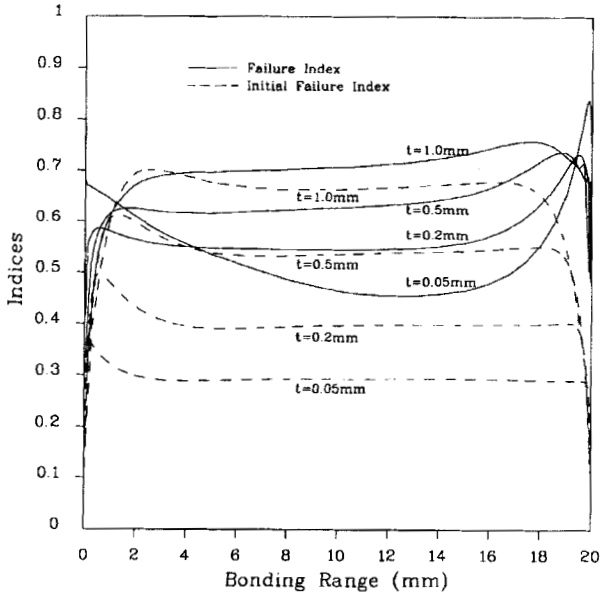

(a)

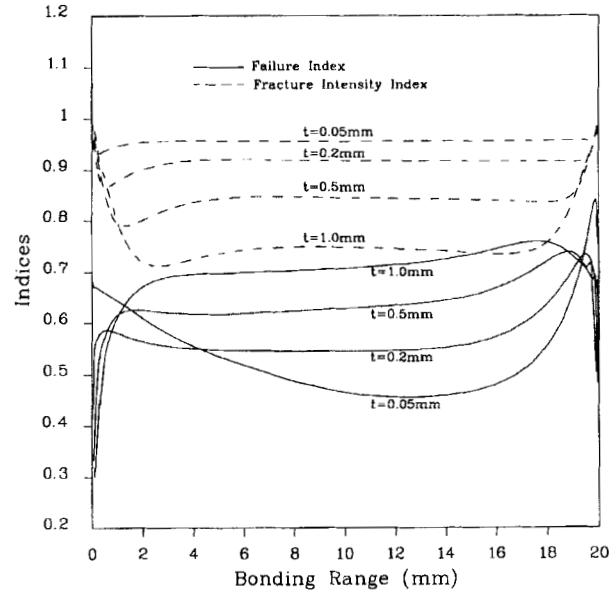

(b)

FIGURE 15 Variations of the initial failure index, k_I, fracture intensity index, k_F, and failure index, k, with respect to the adhesive thickness when the tensile axial load was 15 kN (t: adhesive thickness). (a) Initial failure index, k_I, and failure index, k, (b) Fracture intensity index, k_F, and failure index, k.

CONCLUSIONS

In this work, both the nonlinear mechanical properties and fabrication residual thermal stresses of adhesive were included in the stress analysis of adhesively-bonded tubular single lap steel-steel joints under axial tensile load. The nonlinear tensile properties of adhesive were approximated by an exponential equation which was represented by the initial tensile modulus and ultimate tensile strength of the adhesive.

From the stress analyses and tests of the adhesively-bonded tubular single lap steel-steel joints, the following conclusions were obtained.

(1) The fracture intensity index, k_F, was almost the same as the maximum failure index, k_{max}, calculated with the nonlinear properties of adhesive and residual thermal stresses of fabrication.
(2) The failure of the adhesively-bonded joint occurred when the maximum failure index, k_{max}, was larger than the fracture intensity index, k_F.
(3) The load-bearing capability of the adhesively-bonded joint was greatly influenced by the fabrication residual thermal stresses.
(4) As the adhesive thickness was increased and the load was decreased, the initial failure index, k_I, was increased and approached the failure index, k.
(5) Since the fracture intensity index, k_F, was decreased as the initial failure index, k_I, was increased, it was concluded that the load-bearing capability of the adhesively-bonded tubular single lap steel-steel joint under tensile axial load was decreased as the adhesive thickness was increased.

Acknowledgements

This research was financially supported by Korea Ministry of Science and Technology under the international collaboration research between Korea Advanced Institute of Science and Technology and FRAMASOFT of France.

References

[1] Mallick, P. K., *Fiber-Reinforced Composites* (Marcel Dekker, Inc., New York and Basel, 1988), pp. 417–425.
[2] Kinloch, A. J., *Adhesion and Adhesives* (Chapman and Hall Ltd., New York, 1987), pp. 2–3.

[3] Lubkin, J. L. and Reissner, E., "Stress distribution and design data for adhesive lap joints between circular tubes," *J. Appl. Mechanics, Trans. ASME* **78**, 1213–1221 (1956).
[4] Adams, R. D. and Peppiatt, N. A., "Stress analysis of adhesive bonded tubular lap joints," *J. Adhesion* **9**, 1–18 (1977).
[5] Griffin, S. A., Pang, S. S. and Yang, C., "Strength model of adhesive bonded composite pipe joints under tension," *Polym. Eng. and Sci.* **31**(7), 533–538 (1991).
[6] Shi, Y. P. and Cheng, S., "Analysis of adhesive-bonded cylindrical lap joints subjected to tensional load," *J. Eng. Mechanics* **119**(3), 584–602 (1993).
[7] Terekhova, L. P. and Skoryi, I. A., "Stresses in Bonded Joints of Thin Cylindrical Shells," *Strength Mat.* **4**, 1271–1274 (1979).
[8] Kukovyakin, N. M. and Skoryi, I. A., "Estimating the Strength of Bonded Cylindrical Joints," *Russian Eng. J.* **52**(4), 40–43 (1972).
[9] Harrison, N. L. and Harrison, W. J., "The Stresses in an Adhesive Layer," *J. Adhesion* **3**, 195–212 (1972).
[10] Osswald, T. A. and Rietveld, J., "Measuring Constitutive Properties," in *Adhesives and Sealants* (ASM International, Metals Park, Ohio, 1990), pp. 315–316.
[11] Kim, Y. G., Lee, S. J., Lee, D. G. and Jeong, K. S., "Strength Analysis of Adhesively-Bonded Tubular Single Lap Steel-Steel Joints Under Axial Loads Considering Residual Thermal Stresses," *J. Adhesion* **60**, 125–140 (1997).
[12] Lee, D. G., Kim, K. S. and Lim, Y. T., "An Experimental Study of Fatigue Strength for Adhesively Bonded Tubular Single Lap Joints," *J. Adhesion* **35**, 39–53 (1991).
[13] Carpenter, W. C., "A Comparison of Numerous Lap Joint Theories for Adhesively Bonded Joints," *J. Adhesion* **35**, 55–73 (1991).
[14] Lee, S. J. and Lee, D. G., "Development of a Failure Model for the Adhesively Bonded Tubular Single Lap Joint," *J. Adhesion* **40**, 1–14 (1992).